REPORT DOCUMENTATION PAGE

Form Approved
OMB No. 0704-0188

1. REPORT DATE (DD-MM-YYYY)	2. REPORT TYPE	3. DATES COVERED (From - To)
	Technical Papers	

4. TITLE AND SUBTITLE

Please see attached

5a. CONTRACT NUMBER

5b. GRANT NUMBER

5c. PROGRAM ELEMENT NUMBER

6. AUTHOR(S)

5d. PROJECT NUMBER
1011

5e. TASK NUMBER
0046

5f. WORK UNIT NUMBER
346204

7. PERFORMING ORGANIZATION NAME(S) AND ADDRESS(ES)

Air Force Research Laboratory (AFMC)
AFRL/PRS
5 Pollux Drive
Edwards AFB CA 93524-7048

8. PERFORMING ORGANIZATION REPORT

9. SPONSORING / MONITORING AGENCY NAME(S) AND ADDRESS(ES)

Air Force Research Laboratory (AFMC)
AFRL/PRS
5 Pollux Drive
Edwards AFB CA 93524-7048

10. SPONSOR/MONITOR'S ACRONYM(S)

11. SPONSOR/MONITOR'S NUMBER(S)
Please see attached

12. DISTRIBUTION / AVAILABILITY STATEMENT

Approved for public release; distribution unlimited.

13. SUPPLEMENTARY NOTES

14. ABSTRACT

15. SUBJECT TERMS

16. SECURITY CLASSIFICATION OF:			17. LIMITATION OF ABSTRACT	18. NUMBER OF PAGES	19a. NAME OF RESPONSIBLE PERSON
a. REPORT	b. ABSTRACT	c. THIS PAGE	A		Leilani Richardson
Unclassified	Unclassified	Unclassified			19b. TELEPHONE NUMBER (include area code) (661) 275-5015

4/6

MEMORANDUM FOR PRS (In-House Publication)

FROM: PROI (STINFO) 26 Dec 2001

SUBJECT: Authorization for Release of Technical Information, Control Number: **AFRL-PR-ED-TP-2001-247**
C.W. Larson; W.M. Kalliomaa; F.B. Mead, Jr., "Energy Conversion in Laser Propulsion II"

40th AIAA Aerospace Sciences Meeting & Exhibit **(Statement A)**
(Reno, NV, 13-17 January 2002) (Deadline: 13 Jan 2002)

1. This request has been reviewed by the Foreign Disclosure Office for: a.) appropriateness of distribution statement, b.) military/national critical technology, c.) export controls or distribution restrictions, d.) appropriateness for release to a foreign nation, and e.) technical sensitivity and/or economic sensitivity.
Comments:_____

Signature _____ Date _____

2. This request has been reviewed by the Public Affairs Office for: a.) appropriateness for public release and/or b) possible higher headquarters review.
Comments: _____

Signature _____ Date _____

3. This request has been reviewed by the STINFO for: a.) changes if approved as amended, b) appropriateness of references, if applicable; and c.) format and completion of meeting clearance form if required

Comments:_____

Signature _____ Date _____

4. This request has been reviewed by PR for: a.) technical accuracy, b.) appropriateness for audience, c.) appropriateness of distribution statement, d.) technical sensitivity and economic sensitivity, e.) military/ national critical technology, and f.) data rights and patentability
Comments:_____

APPROVED/APPROVED AS AMENDED/DISAPPROVED

PHILIP A. KESSEL Date
Technical Advisor
Space and Missile Propulsion Division

AIAA 2002-0632
Energy Conversion in Laser Propulsion II.

C. William Larson,
Franklin B. Mead, Jr.,
Wayne M. Kalliomaa

Air Force Research Laboratory
Edwards AFB, CA 93524-7680

40th AIAA Aerospace Sciences Meeting & Exhibit
14-17 January 2002 / Reno, NV

Energy Conversion in Laser Propulsion II
(RenoWorkingDoc.doc – 19 Dec 01)

C. William Larson, Wayne M. Kalliomaa, and Franklin B. Mead, Jr.
Propulsion Directorate
Air Force Research Laboratory
Edwards AFB, CA 93524-7680

Abstract

Analysis of overall energy conversion in laser propulsion is reported. Experimental studies of a laboratory scale propulsion device that absorbs laser energy and converts that energy to propellant kinetic energy were carried out. The Myrabo Laser Lightcraft (MLL), propelled by laser heated air, was studied. The MLL incorporates an inverted parabolic reflector that focuses laser energy into a toroidal volume where it is absorbed by a unit of propellant mass that is subsequently expanded in the geometry of the plug nozzle aerospike. Thermodynamics predicted that the upper limit of the efficiency of conversion of the internal energy of laser heated air to jet kinetic energy, α, is ~ 0.30 for EQUILIBRIUM expansion to 1 bar pressure. The analysis captures the equation of state of partially ionized air under conditions of chemical equilibrium. This upper limit α is nearly independent of the specific internal energy between 1 and 100 MJ/kg, or temperature from 2000 to 24000 K at density of 1.18 kg/m^3. The upper limit efficiency for optimum FROZEN expansion of laser heated air is $\alpha = 0.27$. With heating of air at its Mach 5 stagnation density (5.9 kg/m^3 as compared to STP air density of 1.18 kg/m^3) these efficiencies increase to about 0.55 (equilibrium) and 0.45 (frozen). Optimum blowdown from 1.18 kg/m^3 to 1 bar occurs with expansion ratios ~ 1.5 to 4 as internal energy decreases from 1 to 100 MJ/kg. Heating of Mach 5 air at stagnation density requires larger expansion ratios, 8 to 32, for optimum expansion to 1 bar. Expansion of laser ablated Delrin propellant appears to convert the absorbed laser energy more efficiently to jet kinetic energy because the effective density of the ablated gaseous Delrin is significantly greater than that of STP air.

NOMENCLATURE (in order of use)

E_f	kinetic energy of vehicle at end of mission.
m_f	mass of vehicle at end of mission.
v_f	velocity of vehicle at end of mission in inertial frame of reference.
η	efficiency of conversion of propellant kinetic energy to vehicle kinetic energy.
α	efficiency of conversion of propellant internal energy to propellant kinetic energy.
β	efficiency of absorption of laser energy by propellant.
γ	efficiency of transmission of laser energy through atmosphere to vehicle.
E_L	laser energy per laser pulse.
v_i	initial velocity of rocket in inertial frame, m/s.
v_e	exit velocity of propellant relative to the rocket, in the rocket frame of reference, m/s.
m_i	initial mass of rocket, kg.
f	mass fraction for a rocket mission, $f = m_f/m_i$.
F	Force or thrust of rocket, N = kg m/s^2.
m	mass of rocket, kg.
t	time, s
dm/dt	incremental mass change of rocket, instantaneous propellant mass flow rate, kg/s.
ρ	propellant density, kg/m^3.
$\langle v_e \rangle$	mass weighted average exit velocity of blowdown expansion in rocket frame of reference, m/s.
v	velocity of rocket in inertial frame of reference, m/s.
dv/dt	incremental velocity change of rocket in the inertial frame of reference, m/s^2.
x	ratio of $v_f - v_i$ to v_e.
y	ratio of v_i to v_e.
E_p	kinetic energy of propellant, J.
$\langle v_e^2 \rangle$	mass weighted average squared exit velocity of propellant in a blowdown expansion, m^2/s^2.
m_p	mass of propellant, kg.

I	impulse, Ns = kg m/s.
C	coupling coefficient, Ns/J.
Φ	ratio of square of mass weighted average exit velocity to mass weighted root mean square exit velocity, $\langle v_e \rangle^2 / \langle v_e^2 \rangle$.
u_c	specific internal energy of laser heated propellant, J/kg.
u°	specific internal energy of propellant before laser heating, u°_{air} at STP = - 9.0 x 10^4 J/kg.
u_e	specific internal energy of propellant at the exit of the rocket after isentropic expansion.
V_{abs}	absorption volume.
V_{abs}^*	normalized absorption volume, $V_{abs}^* = V_{abs}/\beta$.
C^*	normalized coupling coefficient, $C^* = C/\beta$.
v_e^*	normalized exit velocity, $v_e^* = \langle v_e \rangle / \beta\Phi$.
$(u_c-u^\circ)^*$	normalized specific internal energy, $(u_c-u^\circ)^* = (u_c-u^\circ)/\beta^2\Phi$.
T	temperature, K.
P	pressure, bar.
h	specific enthalpy, J/kg.
s	specific entropy, J/kg K.
M_m	average molecular weight of a mixture, g/mole.
c_p	specific heat capacity at constant pressure.
v_a	velocity of sound, m/s.
X(e-)	mole fraction of electrons.
ε	expansion ratio
A_e	area of exit surface
A_t	area of sonic surface or throat area

Subscripts, Acronyms, symbols

i	initial value of property.
f	final value of property.
c	property in chamber
t	property in throat
e	property in exit plane
p	property of propellant
<x>	denotes mass weighted average of x
HELSTF	High Energy Laser System Test Facility
PLVTS	Pulsed Laser Vulnerability Test System
MLL	Myrabo Laser Lightcraft
STP	Standard Temperature and Pressure, 298 K, 1.01326 bar

INTRODUCTION

Laser propulsion is limited by laser power, so optimization of the laser propulsion mission may be factored into optimization of four energy conversion efficiencies, which, in a first approximation, are independent of each other. In this idealization the kinetic energy of the propelled vehicle at the end of the mission may be expressed simply:

$$(1) \qquad E_f = \tfrac{1}{2} m_f v_f^2 = \eta\alpha\beta\gamma E_L.$$

The "propulsion efficiency", η, is the efficiency with which jet kinetic energy is converted into vehicle kinetic energy. Sutton[1] pointed out, more than 50 years ago, that the instantaneous propulsion efficiency varies during a rocket mission and that it is unity only when the vehicle velocity in the inertial frame is equal to the jet velocity in the rocket frame. Thus, unit propulsion efficiency is achieved only when the jet is deposited as a stationary mass relative to an observer in the inertial frame of reference.

Then, 25-years ago, Moeckel[2] and Lo[3] independently and nearly simultaneously published analyses of the optimization of laser rocket propulsion by maximizing the overall mission average efficiency of conversion of jet

kinetic to vehicle kinetic energy. Most recently, Phipps, Reilly and Campbell (2000, 2001)[4] cited Moeckel's paper in their comprehensive analysis of the single stage, constant I_{sp} Earth to LEO rocket mission. They reiterated the fundamental limit that Newton's second law imposes: for rocket missions that start at zero initial velocity, the maximum η is 0.648, which is achieved when $f = 0.203$ and $v_f/v_e = 1.595$. For the Earth to LEO mission the effective "delta v" (v_f) is about 10 km/s, so the optimum single stage to orbit jet velocity is ~ 6.27 km/s, or specific impulse ~ 640 s.

In this paper we report a continuation of our previous work[5] and report detailed thermodynamics analysis of energy conversion in the "blowdown" of laser heated air via the path that minimizes entropy increase. The results derive from analysis of isentropic expansions from chemically equilibrated states that may be specified by their internal energy, density, and overall stoichiometry. Under conditions of chemical equilibrium the mixture composition adjusts itself to minimize the Gibbs free energy, or chemical potential. The accuracy of the equlibrium composition depends on the accuracy of specification of relevant species in the mixture and their thermodynamic properties. The analysis spans a temperature range of 2000 to 24000 K, and several orders of magnitude in pressure.

We discuss and analyze measurements of the overall efficiency of conversion of laser energy to propellant kinetic energy, $\alpha\beta$, based on various ballistic pendulum and flight experiments with Myrabo Laser Lightcraft, MLL [Messitt, Myrabo, and Mead (2000)[6]; Mead, Squires, Beairsto, and Thurston (2000)[7]]. The Phipps, et al.[4] study defined an "ablation efficiency " and analyzed the Earth to LEO mission with unit ablation efficiency. Their ablation efficiency is equivalent to the product of our α and β. By analyzing experimental results, we are able to narrow the range of β that operates during the heating process. These β values are somewhat larger than those reported by Wang, et al.[8] for CFD plasma models of the heating process. It has been pointed out that β approaches zero as the plasma temperature approaches ~ 40,000 K, where the plasma frequency approaches the laser frequency.[8, 9]

The Rocket Equation

The thrust that results from expulsion of matter at velocity v_e from a vehicle of mass m is expressed by Newton's second law as

$$(2) \qquad \mathbf{F} = -\frac{d(mv_e)}{dt},$$

where mv_e is the momentum of the jet exhaust in the vehicle frame of reference, [Corliss, (1960)][10]. For the case where v_e is constant,

$$(3) \qquad \mathbf{F} = -v_e \frac{dm}{dt}.$$

Equation (2) may also be used to define an average exit velocity for rockets where v_e is not constant, such as blowdown of a specified mass of hot propellant from a fixed volume, e.g., as in laser rockets and pulse detonation rockets:

$$(4) \qquad \langle v_e \rangle = -\frac{\int_0^t F dt}{\int_{m_i}^{m_f} dm} = \frac{\int_{m_i}^{m_f} d(m v_e)}{\int_{m_i}^{m_f} dm} = \frac{\int_{\rho_i}^{\rho_f} d(\rho v_e)}{\int_{\rho_i}^{\rho_f} d\rho}.$$

so that $\langle v_e \rangle$ is the mass weighted average exit velocity. Chemical thermodynamics may be used to rigorously establish upper limits of $\langle v_e \rangle$ when the propellant equation of state is known and the initial and final states of the propellant expansion are specified.

The Rocket Equation results from a balance of the force exerted by the propellant on the vehicle and the motion of the vehicle under the influence of the propulsive force as required by Newton's second law. Thus, in the absence of other forces, such as body (gravitational) force and drag force,

$$(5) \qquad F = -v_e \frac{dm}{dt} = m \frac{dv}{dt}.$$

where v is the vehicle velocity in the inertial frame of reference, i.e., the velocity relative to a fixed point in space. Elimination of time in Equation (5) yields the expression for conservation of momentum, $mdv = -v_e dm$, which may be integrated between the limits of initial and final mission velocity (v_i and v_f) and mass (m_i and m_f) to produce the Rocket Equation,

$$(6) \qquad f = \frac{m_f}{m_i} = \exp -\left[\frac{v_f - v_i}{v_e}\right] = \exp(-x).$$

Overall Efficiency of Conversion of Laser Energy to Propellant Kinetic Energy, $\alpha\beta$

The efficiency of conversion of laser energy to propellant kinetic energy may be defined by energy conservation for the general case of variable v_e such as occurs with blowdown expansion of laser heated air.

$$(7) \qquad E_p = \tfrac{1}{2} m_p \langle v_e^2 \rangle = \alpha\beta E_L,$$

where the mass weighted average of the square of the propellant exit velocity is

$$(8) \qquad \langle v_e^2 \rangle = \frac{\int_{\rho_e}^{\rho_f} d(\rho v_e^2)}{\int_{\rho_e}^{\rho_f} d\rho}.$$

The impulse, $I = \int F dt$, imparted to a test article by expansion of its propellant may be accurately measured with a ballistic pendulum. Momentum conservation requires equivalence between the measured impulse and the propellant impulse so that

$$(9) \qquad I = m_p \langle v_e \rangle.$$

The momentum coupling coefficient, also a measured quantity, is the impulse imparted to a test article per unit laser energy incident on the propellant,

$$(10) \qquad C = \frac{I}{E_L}.$$

Using the definitions embodied in Equations (7) – (10), C may be expressed in terms of α, β, $\langle v_e \rangle$, and $\langle v_e^2 \rangle$:

$$(11) \qquad C = \frac{2\alpha\beta}{\langle v_e \rangle}\left[\frac{\langle v_e \rangle^2}{\langle v_e^2 \rangle}\right] = \frac{2\alpha\beta\Phi}{\langle v_e \rangle}$$

If v_e is constant, $\Phi = \langle v_e \rangle^2 / \langle v_e^2 \rangle = 1$. Thermodynamics may be used to rigorously establish inviolate upper limits to Φ and α for any specified free-expansion blowdown process when the propellant equation of state is known. The Φ factor depends on the mass distribution of exit velocities, and is mathematically limited to $0.5 \leq \Phi \leq 1$. It will be shown (Figure 6, *vide infra*) that Φ for optimum blowdown of laser heated air to 1 bar pressure increases from 0.95 at low energy (2 MJ/kg) to 0.98 at high energy (60 MJ/kg). The Φ factor arises in Equation (11) because the measured quantity, the jet impulse, is proportional to mass weighted average velocity whereas the jet kinetic energy is proportional to the mass weighted average of the squared velocity.

Experimental determination of $\alpha\beta$

The value of $\alpha\beta$ may be determined within a factor of $\Phi \leq 1$ by experimental measurement of the impulse imparted to a test article (**I**) when a laser pulse of known energy (E_L) ejects a known amount of propellant mass (m_p):

$$(12) \qquad \alpha\beta\Phi = \frac{I^2}{2m_pE_L} = \frac{CI}{2m_p} = \frac{C\langle v_e\rangle}{2} = \frac{I\langle v_e\rangle}{2E_L}.$$

Thus, measurement of $\alpha\beta$ requires knowledge of the propellant mass that is associated with the measured impulse and laser pulse energy. In the absence of a mass measurement, a lower limit to propellant mass and an upper limit to exit velocity may be established. Since $\beta \leq 1$ is required for energy conservation,

$$(13) \qquad m_p \geq \frac{I^2}{2\alpha\Phi E_L}, \text{ and}$$

$$(14) \qquad v_e \leq \frac{2\alpha\Phi E_L}{I}.$$

Use of thermodynamics to establish upper limits to Φ and α enables additional restrictions to be placed on the permissible experimental values of the upper limit v_e and lower limit m_p.

Maximum Efficiency of Conversion of Propellant Internal Energy to Propellant Kinetic Energy, α.

In the analysis of idealized thermodynamic expansion of laser heated air, the notion of an energy absorption volume is invoked that contains a mass of propellant $m_p = \rho_c V_{abs}$ into which an amount of energy βE_L is deposited. The time scale for energy absorption is much shorter than that for expansion so that the propellant density within V_{abs} (the chamber) remains constant during energy absorption. This enables the initial specific internal energy of the propellant to be defined,

$$(15) \qquad u_c - u^o = \beta E_L/\rho_c V_{abs},$$

where $\rho_c = 1.18$ kg/m^3 and $u^o = 0.09 \times 10^6$ J/kg for air at STP. Table 1 provides a convenient list of values of the normalized absorption volume, $V_{abs}^* = V_{abs}/\beta$, derived from Equation (15) for various values of $u_c - u^o$ and E_L.

Figure 1 shows a cross-section of the test article with a ring of Delrin installed in the shroud. The Delrin shown occupies a volume of 7 cm^3, which may be used to visualize a reasonable absorption volume for the case where Delrin is absent and air is the heated material. Table 1 shows that a similar absorption volume for air would produce, with unit β and nominal E_L values between 100 and 400 J, heated air with 10 to 40 MJ/kg internal energy. If the Delrin surface shown in the figure, about 25 cm^2, is a suitable representation of the sonic surface of expanding air, then, with an idealized plug-nozzle exit area[11] of ~ 350 cm^2, the expansion ratio in this test article may be as large as ~ 14.

Perfect isentropic conversion of internal energy to propellant kinetic energy occurs with no losses so that

$$(16) \qquad \langle v_e^2\rangle = 2\langle u_c - u_e\rangle = 2\alpha(u_c - u^o), \text{ where}$$

$$(17) \qquad \alpha = \langle u_c - u_e\rangle/(u_c - u^o) = \langle v_e^2\rangle/2(u_c - u^o), \text{ and}$$

$$(18) \qquad \langle v_e\rangle = 2\langle (u_c - u_e)^{1/2}\rangle.$$

These definitions generate a second expression for **C** in terms of the specific energy of laser heated propellant:

$$(19) \qquad \mathbf{C} = \beta\,[2\alpha\Phi/(u_c - u^o)]^{1/2}.$$

Figure 2 shows the relationships between six variables of interest: **C**, α, β, Φ, $\langle v_e \rangle$, and $[u_c - u^o]$ that derive from definitions given by Equations (11) and (19). The Figure shows $\mathbf{C}^* = \mathbf{C}/\beta$ vs α plot with lines of constant $\langle v_e \rangle^* = \langle v_e \rangle/\Phi$ and lines of constant $(u_c - u^o)^* = (u_c - u^o)/\Phi$. As one proceeds from the origin along a paraboloidal line of constant $(u_c - u^o)^*$, which is also a line of constant entropy, both $\mathbf{C}^*$ and α increase. At constant α, $\mathbf{C}^*$ decreases as $\langle v_e \rangle^*$ and $(u_c - u^o)^*$ increase. Knowledge of **C** and α fixes values of $\langle v_e \rangle/\beta\Phi$ and $[u_c - u^o]/\beta^2\Phi$. Figure 1 may also be interpreted as a **C** vs α plot with lines of constant $\langle v_e \rangle/\beta\Phi$ and lines of constant $[u_c - u^o]/\beta^2\Phi$. The absorption volume may also be factored into this parameter space with use of Equation (15) or Table 1.

Thermodynamic Limitations to α and Φ.

Figure 3 shows the chemical equilibrium Mollier diagram for air up to 24,000 K. Figure 3 is based on the database maintained at NASA/Glenn [McBride and Gordon (1996)][12], which is certified accurate up to 20,000 K and which is based on extended 9-parameter fits to enthalpy, heat capacity, and entropy of neutral species and singly charged ions. Above 20,000 K doubly charged ions begin to contribute but these are not included in the database. This limitation leads to predictions of temperatures (at specified u and ρ) that are too high for plasmas above ~ 20,000 K.

Figure 4 shows a series of vertical lines on the Mollier diagram. These are representations of equilibrium isentropic expansions that originate from initial states located along the constant density line, $\rho = 1.18$ kg/m^3, and specific internal energies ranging from 1 to 100 MJ/kg. Table 2 summarizes other thermodynamic properties of these initial equilibrium states of interest: T, P, h, s, M_m, c_p, v_a, c_p/c_v, and $X(e^-)$. Table 3 provides a similar summary of properties for the case of Mach 5 air at its stagnation density[13], 5.9 kg/m^3. Since the entropy of the initial and final states are equal, the thermodynamic state of the propellant in the exit surface is uniquely defined when only one additional property in the exit surface is specified, such as the exit pressure or the expansion ratio, which are indicated in Figure 4. The expansion ratio, ε, is the ratio of the area of the exit surface to the area of the sonic surface or nozzle throat, and for isentropic expansions this may be represented in terms of thermodynamic properties in the nozzle throat and exit plane: $\varepsilon = A_e/A_t = \rho_t v_a/\rho_e v_e$.

Optimum Blowdown to $P_a = 1$ bar. Mass Weighted Average Quantities

Figure 5 shows a representation of blowdown from the initial state where $u_c - u_o = 2E3$ kJ/kg and the initial density is that of STP air. The series of vertical lines are located at equally spaced density increments. The instantaneous and mass weighted average quantities based on Equations (16) – (19) are shown in Figures 6 – 9.

Figures 10 and 11 show the transformations of the isentropes in the Mollier plane (u-s plane) to the $\mathbf{C}^*$-α plane. Lines of constant ε and ρ_e are almost exactly coincident. Lines of constant exit pressure run nearly parallel to lines of constant ε and ρ_e, and all are nearly vertical, indicating that alpha is nearly independent of v_e and $u_c - u^o$.

DISCUSSION

Coupling coefficients measured with the Figure 1 test model were reported in our previous paper[5]. With increasing laser energy they rise to plateaus above about 300 J. At $E_L \sim 300$ J, C(Delrin) ~ 350 Ns/MJ and the ablated/vaporized mass was $m_p \sim 35$ mg. This means that $\langle v_e \rangle \sim 3000$ m/s by Equations (9) and (10), and $\alpha\beta\Phi \sim 0.5$ by Equation (11). Thus, $\alpha > 0.5$, which is remarkably high. Air and Delrin will show very similar expansion behavior. As shown by Figure 11, the dependence of α on the density of the heated air is quite strong. At $[u_c - u^o]^* = 10$ MJ/kg and expansion to 1 bar, Figure 11 shows that the instantaneous α increases from about 0.43 to about 0.60 when the density increases from the STP value (1.18 kg/m^3) to its Mach 5 stagnation value (5.9 kg/m^3). The instantaneous α values decrease to about 0.32 and 0.5 respectively when the mass weighted average α for the free-expansion blowdown process is calculated. An α value around 0.5 is reasonable when the density of the ablated and vaporized delrin is as high as ~ 6 kg/m^3 and the blowdown expansion is near perfect. Most importantly, it appears that most of the inefficiency in the composite $\alpha\beta\Phi$ efficiency is carried by α and that $\beta\Phi$ is very close to unity.

Coupling coefficients at $E_L > 300$ J for air were found to depend strongly on the quality of the laser beam, as between a tightly focused beam that produced lower $\mathbf{C} \sim 100$ Ns/MJ than a loosely focused beam, which produced $\mathbf{C} \sim 150$ Ns/MJ. This may be due to the tight beam heating a smaller mass of air to a higher energy than

the more diffuse loosely focused beam. Although the exit velocity would be higher in the tight beam case, the total impulse may be lower because the heated mass is lower. Figure 1 shows the geometry and size relationship of a 7 cm^3 absorption volume inside the shroud, which contains ~ 8 mg of air. With **C**(air, loose focus) = 150 Ns/MJ at E_L = 300 J, and m_p = 8 mg we may deduce $\langle v_e \rangle \sim 5600$ m/s, and $\alpha\beta\Phi \sim 0.42$. If the absorption volume is double, then $\langle v_e \rangle$ and $\alpha\beta\Phi$ are halved. Figure 10 shows that air heated to 10 MJ/kg for example would blowdown to 1 bar with $\alpha = 0.32$ (equilibrium expansion) or $\alpha = 0.27$ (frozen expansion).

If we accept that a reasonable upper limit operational alpha is ~ 0.30 in our experiments $\alpha < 0.3$, then the measured **C** ~ 150 Ns/MJ and Equation (9-11) with $\beta\Phi = 1$ require $\langle v_e \rangle < 4000$ m/s, and $m_p > 11$ mg. Now if $\beta\Phi$ is ~ 0.3 as has been suggested by CFD modeling,[8] then the upper limit of $\langle v_e \rangle$ decreases to 1200 m/s and the lower limit of m_p increases to 36 mg. It would seem apparent that the value of β is somewhat larger than 0.3 because both the upper limit $\langle v_e \rangle$ and lower limit m_p are not reasonable for the geometry shown in Figure 1.

CONCLUSIONS

Experimental studies of the 200-3/4 model Myrabo Laser Lightcraft with air heated by 10.6 μ radiation from a CO_2 laser showed that energy conversion efficiencies of laser energy to propellant kinetic energy were at least 30%. This was found to be consistent with highly simplified analysis of equilibrium (isentropic) expansions from initial states that are specified by a single parameter, the volume into which the laser energy is absorbed. The measured exit velocity based on estimated air mass is in the neighborhood of 3000 m/s. It should be noted that beam quality plays an important role in the performance of the model 200-3/4 MLL which is counterintuitive inasmuch as lower beam quality (energy spread over a larger area) produces higher **C** coupling coefficients. Computational fluid dynamics modeling of the absorption (and reflection) of laser energy and expansion of the formed plasma[8] have recently been carried out. The simple analysis presented here may only be useful in providing upper limitations to the conversion of laser energy to propellant kinetic energy and to provide a simplified visualization and description of the processes occurring in blowdown of laser heated propellants in MLL devices.

Expansion of a propellant mass that was heated at constant volume was examined under conditions where either chemical equilibrium or frozen composition was maintained. For expansion with an effective area ratio of ~ 4, which is appropriate for the MLL, a maximum of 25 to 50% of the internal energy is predicted to be convertible to propellant kinetic energy, based on the minimization of the entropy gain of the blowdown process. With the small effective area ratio ~ 4, equilibrium expansion was only slightly more efficient than frozen expansion. Heating of propellant to highly ionized states resulted in lower efficiency energy conversion but higher exit velocity. The thermodynamic limitations are illustrated by process representations of blowdown in the Mollier plane.

REFERENCES

1. Sutton, George P., "Rocket Propulsion Elements, An Introduction to the Engineering of Rockets," (John Wiley and Sons, Inc., copyright 1949), page 17. See also: Sutton, George P., and Biblarz, Oscar, "Rocket Propulsion Elements, Seventh Edition," (John Wiley and Sons, Inc., New York, copyright 2001). page 38.
2. Moeckel, W. E., "Optimum exhaust velocity for laser-driven rockets," J. Spacecraft, Vol. 12, No. 11, Pages 700-701, manuscript received May 12, 1975, revision received July 11, 1975. Shows derivation of deltaV/Vexit = 1.5936.
3. Lo, R. E., "Propulsion by laser energy transmission (considerations to selected problems)," IAF PAPER 76-165, October 1, 1976, 11 pages.
4. Phipps, C. R, Reilly, J. P., and Campbell, J. W., "Optimum parameters for laser-launching objects into low earth orbit," *Lasers and Particle Beams*, **18**(1), (2001), pp 1-35. See also: Phipps, C. R, Reilly, J. P., and Campbell, J. W., "Laser launching a 5-kg object into low earth orbit," Presented at the Third International Symposium on High Power Laser Ablation, Santa Fe, NM, 23-28 April 2000, *Proceedings of SPIE* **4065**, 502 (2000).
5. Larson, C. W., and Mead, F. B. Jr., "Energy Conversion in Laser Propulsion," 39th AIAA Aerospace Sciences Meeting, 8-11 January 2001, Reno, NV, Paper No. 2001-0646.
6. Messitt, Donald G., Myrabo, Leik N. and Mead, Franklin B. Jr., "Laser initiated blast wave for launch vehicle propulsion," 36th AIAA Joint Propulsion Conference, 16-19 July 2000, Huntsville, AL, paper 2000-3035.
7. Mead, Franklin B. Jr., Squires, Stephen, Beairsto, Chris, and Thurston, Mike, "Flights of a laser-powered Lightcraft during laser beam hand-off experiments," 36th AIAA Joint Propulsion Conference, 16-19 July 2000, Huntsville, AL, paper 2000-3484.

8. Wang, Ten-See, Mead, Franklin B. Jr., and Larson, Carl W., "Analysis of the Effect of Pulse Width on Laser Lightcraft Performance," 37th AIAA Joint Propulsion Conference, 8-11 July 2001, Salt Lake City, UT, Paper No. 2001-3664. See also: Liu, Jiwen, Chen, Yen-Sen, and Wang, Ten-See, "Accurate prediction of radiative heat transfer in laser induced air plasmas," 34th AIAA Thermophysics Conference, 19-22 June 2000, Denver, CO, paper 2000-2370. See also: Wang, Ten-See, Chen, Yen-Sen, Liu, Jiwen, Myrabo, Leik N., and Mead, Franklin B. Jr., "Advanced Performance Modeling of Experimental Laser Lightcrafts," 39th AIAA Aerospace Sciences Meeting and Exhibit, 8-11 January 2001, Reno, NV, Paper 2001-0648.
9. Pakhomov, Andrew V., and Gregory, Don A., "Ablative Laser Propulsion: An Old Concept Revisited," AIAA Journal, April 2000, Vol 38, Issue 4, p 725.
10. Corliss, William R., "Propulsion Systems for Space Flight," McGraw-Hill Book Company, 1960.
11. Vinson, John, "Aerospike engine design gains new thrust," Aerospace America, February 1998, pp.30-33. See also: Weegar, Richard, "Understanding External Expansion Engines," Launchspace Magazine, August 1996, p. 1719.
12. McBride, Bonnie J., and Gordon, Sanford, "Computer program for calculation of complex chemical equilibrium compositions and applications, II. Users manual and program description," NASA Reference Publication 1311, Lewis Research Center, Cleveland, OH 44135, June 1996.
13. Shapiro, Ascher H., "The Dynamics and Thermodynamics of Compressible Fluid Flow, Volume 1," Ronald Press, New York, N. Y., copyright 1953, page 625.

Table 1. Normalized absorption volume for air at 1.18 kg/m^3 as a function of internal energy and laser energy.

u	V_{abs}/β, normalized absorption volume, cm^3					
MJ/kg	E_L=50 J	E_L=100 J	E_L=150 J	E_L=200 J	E_L=300 J	E_L=400 J
1	42.3	84.7	127.1	169.4	254.2	338.9
2	21.1	42.3	63.5	84.7	127.1	169.4
3	14.1	28.2	42.3	56.5	84.7	112.9
4	10.5	21.1	31.7	42.3	63.5	84.7
5	8.47	16.9	25.4	33.9	50.8	67.8
6	7.06	14.1	21.1	28.2	42.3	56.5
7	6.05	12.1	18.1	24.2	36.3	48.4
8	5.30	10.5	15.8	21.1	31.7	42.3
9	4.71	9.42	14.1	18.8	28.2	37.6
10	4.24	8.47	12.7	16.9	25.4	33.9
15	2.82	5.65	8.47	11.3	16.9	22.6
20	2.12	4.24	6.36	8.47	12.7	16.9
30	1.41	2.82	4.24	5.65	8.47	11.3
40	1.06	2.12	3.18	4.24	6.36	8.47
50	0.85	1.69	2.54	3.39	5.08	6.78
60	0.71	1.41	2.12	2.82	4.24	5.65
70	0.61	1.21	1.82	2.42	3.63	4.84
80	0.53	1.06	1.59	2.12	3.18	4.24
90	0.47	0.94	1.41	1.88	2.82	3.77
100	0.42	0.85	1.27	1.69	2.54	3.39
110	0.39	0.77	1.16	1.54	2.31	3.08

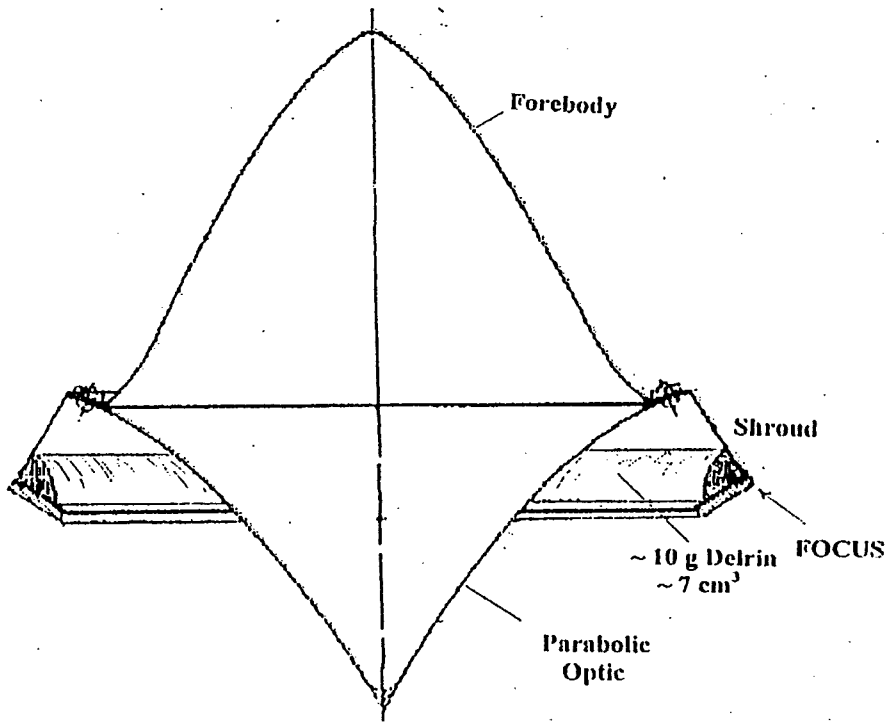

Figure 1. Cross-sectional view of Myrabo Laser Lightcraft, Model 200-3/4. The maximum diameter of the test article at the shroud is ~ 10 cm. The indicated ring of Delrin weighs ~ 10 g and has a volume of ~ 7 cm^3 and a surface area ~ 25 cm^2. The idealized plug nozzle exit area is ~ 350 cm^2.

Table 2. Thermodynamic properties of equilibrium air, $\rho = 1.18$ kg/m^3.

u	T	P	h	s	c_p	M_m	X(e$^-$)	v_a	c_p/c_v
MJ/kg	10^3 K	bar	MJ/kg	KJ/kg K	KJ/kg K	kg/kmol		km/s	
-0.9	0.298	1.000	-.004	6.864	1.005	28.965	0	0.346	1.40
1	1.6	5.4	1.5	8.2	1.25	29.0	4E-10	0.77	1.30
2	2.5	8.6	2.7	8.7	1.51	28.9	3.E-09	0.95	1.24
3	3.2	11.1	3.9	9.0	2.16	28.6	3.E-08	1.06	1.20
4	3.7	13.1	5.1	9.3	2.83	27.8	3.E-07	1.15	1.19
5	4.1	15.0	6.3	9.6	3.15	26.9	2.E-06	1.23	1.19
6	4.5	16.9	7.4	9.8	3.04	26.1	5.E-06	1.32	1.21
7	4.9	19.1	8.6	10.0	2.69	25.3	2.E-05	1.41	1.23
8	5.4	21.5	9.8	10.2	2.56	24.7	4.E-05	1.50	1.23
9	5.9	23.9	11.0	10.4	2.86	24.2	8.E-05	1.57	1.21
10	6.3	26.0	12.2	10.6	3.43	23.8	1.E-04	1.62	1.19
15	7.5	34.1	17.9	11.3	6.70	21.7	5.E-04	1.84	1.17
20	8.3	41.3	23.5	11.9	8.93	19.8	9.E-04	2.02	1.17
30	9.7	56.2	34.8	13.0	9.09	16.9	3.E-03	2.38	1.19
40	11.5	75.4	46.4	14.0	5.13	15.0	1.E-02	2.81	1.24
50	14.4	101.0	58.5	14.8	4.81	14.0	4.E-02	3.26	1.25
60	16.6	124.0	70.5	15.4	6.62	13.2	1.E-01	3.60	1.24
70	18.4	145.0	82.3	16.0	8.25	12.4	1.E-01	3.91	1.24
80	19.9	167.0	94.1	16.5	9.51	11.7	2.E-01	4.20	1.24
90	21.3	189.0	106.0	17.0	10.40	11.1	2.E-01	4.48	1.25
100	22.6	211.0	118.0	17.4	10.90	10.5	3.E-01	4.76	1.26
110	23.9	235.0	130.0	17.9	11.10	10.0	3.E-01	5.03	1.27

Table 3. Thermodynamic properties of Mach 5 air at stagnation density, $\rho = 5.90$ kg/m^3.

u	T	P	h	s	c_p	M	X(e$^-$)	v_a	c_p/c_v
MJ/kg	10^3 K	bar	MJ/kg	KJ/kg K	KJ/kg K	kg/kmol		km/s	
0.102	0.560	9.492	0.263	6.864	1.042	28.965	0	0.471	1.38
1	1.6	27.1	1.5	7.7	1.25	28.97	4e-13	0.77	1.30
2	2.6	43.2	2.7	8.2	1.45	28.95	6.E-11	0.96	1.25
3	3.3	56.5	4.0	8.6	1.85	28.73	2.E-08	1.08	1.21
4	3.9	67.7	5.1	8.9	2.33	28.19	3.E-07	1.17	1.20
5	4.4	78.2	6.3	9.1	2.65	27.46	2.E-06	1.26	1.20
6	4.8	88.9	7.5	9.3	2.71	26.69	6.E-06	1.35	1.22
7	5.3	100.3	8.7	9.5	2.61	25.96	2.E-05	1.45	1.23
8	5.8	112.4	9.9	9.7	2.55	25.32	4.E-05	1.53	1.23
9	6.3	124.5	11.1	9.9	2.69	24.79	8.E-05	1.61	1.22
10	6.7	135.8	12.3	10.0	3.04	24.32	1.E-04	1.67	1.21
15	8.2	182.0	18.1	10.7	5.49	22.19	6.E-04	1.91	1.18
20	9.2	222.3	23.8	11.2	7.36	20.32	1.E-03	2.11	1.18
30	10.8	304.9	35.2	12.2	8.05	17.41	3.E-03	2.49	1.20
40	12.7	404.9	46.9	13.1	5.52	15.45	1.E-02	2.92	1.24
50	15.6	534.8	59.1	13.8	4.28	14.33	3.E-02	3.39	1.27
60	18.4	667.9	71.3	14.4	5.20	13.54	8.E-02	3.78	1.26
70	20.8	794.6	83.5	14.9	6.32	12.81	1.E-01	4.13	1.27
80	22.8	919.9	95.6	15.4	7.26	12.14	2.E-01	4.45	1.27
90	24.6	1046.6	107.7	15.8	7.99	11.52	2.E-01	4.76	1.28

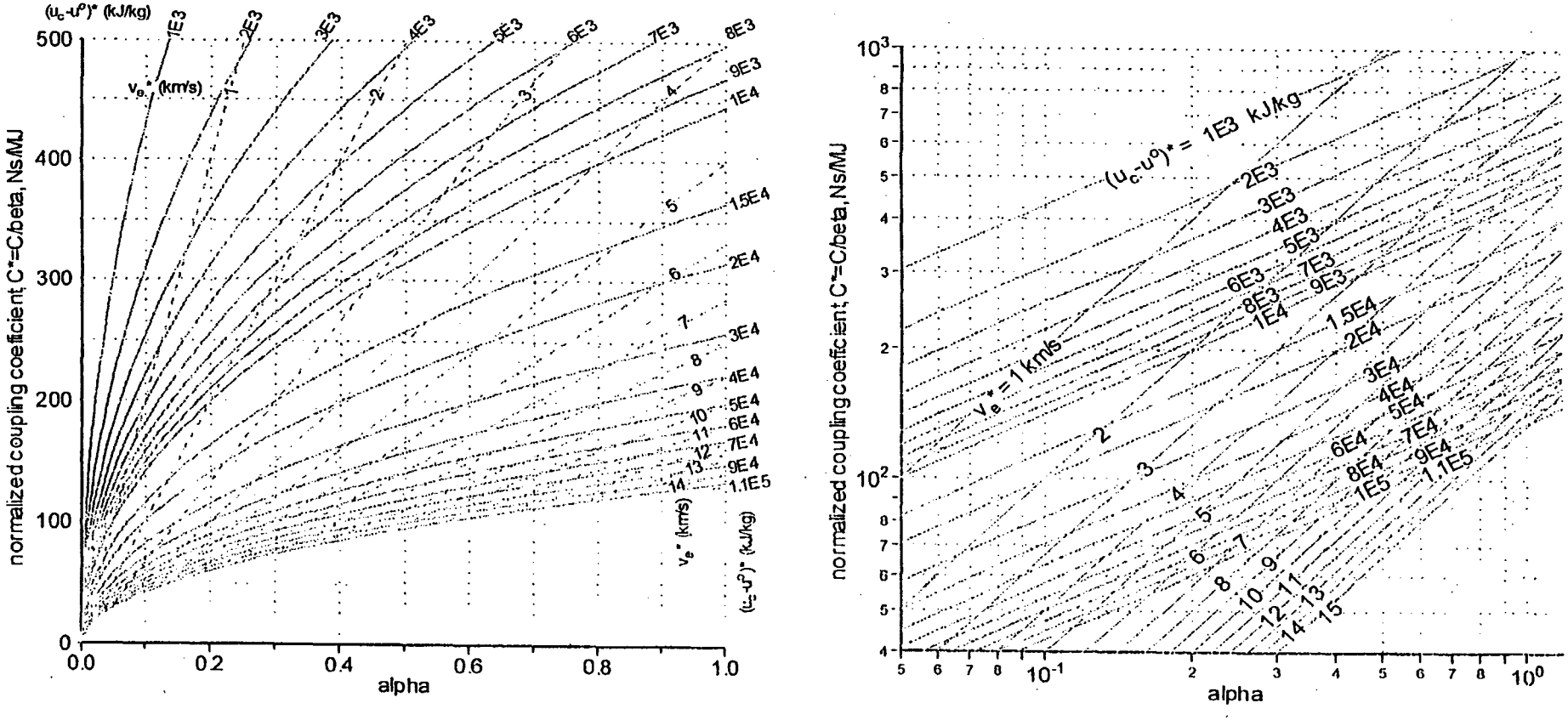

Figure 2. Defined relationships between six variables of interest: C^*, α, β, Φ, $\langle v_e \rangle^*$, and $[u_c - u^o]^*$. The plots show $C^* = C/\beta$ as a function of α, with lines of constant $v_e^* = \langle v_e \rangle/\Phi$ and constant $[u_c\text{-}u^o]^* = [u_c\text{-}u^o]/\Phi$. The plots may alternatively be interpreted as a C vs α plots with lines of constant $v_e^* = \langle v_e \rangle/\beta\Phi$ and constant $[u_c\text{-}u^o]^* = [u_c\text{-}u^o]/\beta^2\Phi$.

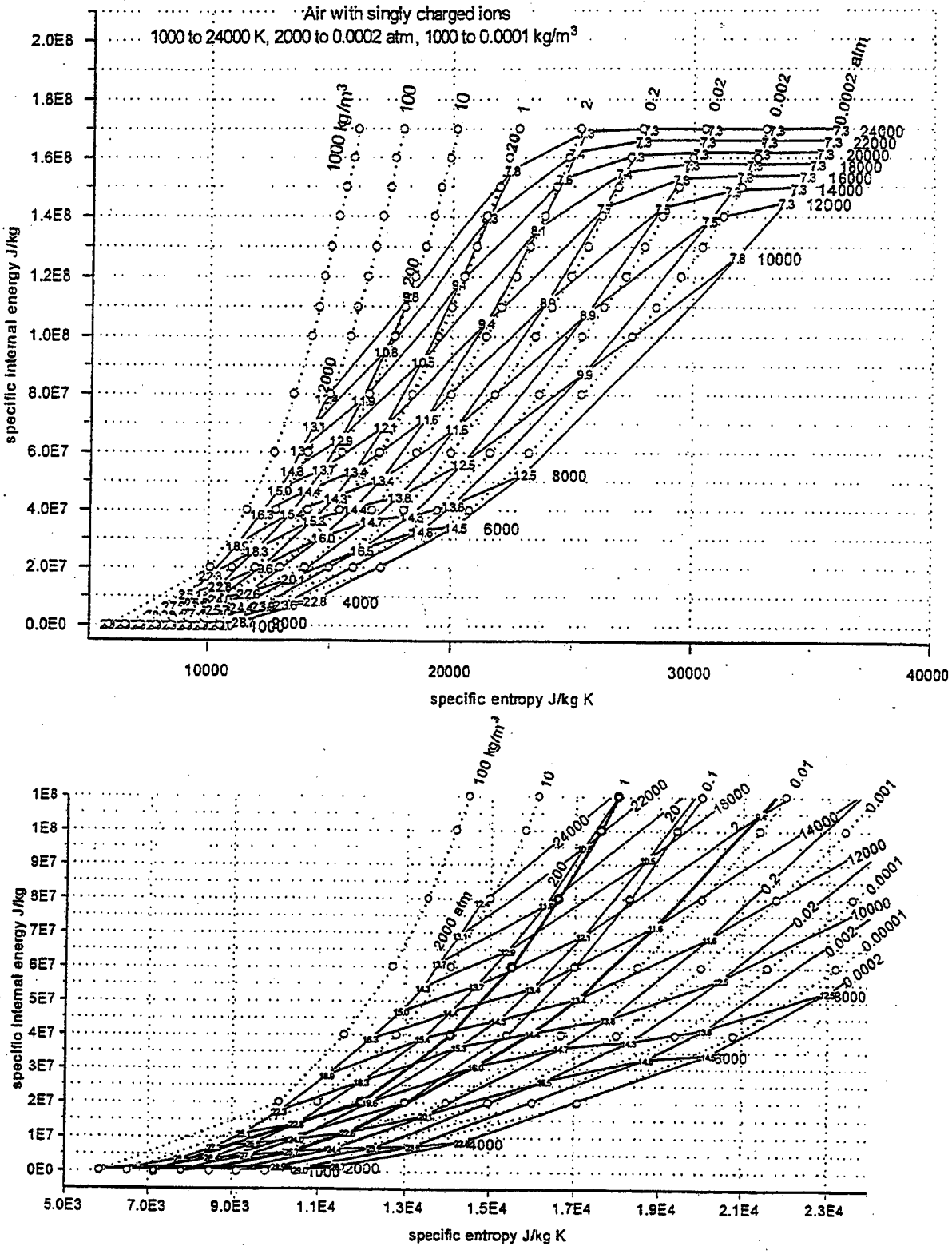

Figure 3. Mollier diagram for air including singly ionized species. Molecular weights are indicated at intersections of isobars and isotherms. The lower diagram shows a heavy constant density line, $\rho = 1.18$ kg/m^3 above a heavy constant pressure line, $P = 1$ atm. The maximum energy initial states of laser heated STP air lie on the constant density line and the optimally expanded states lie vertically below on the constant pressure line.

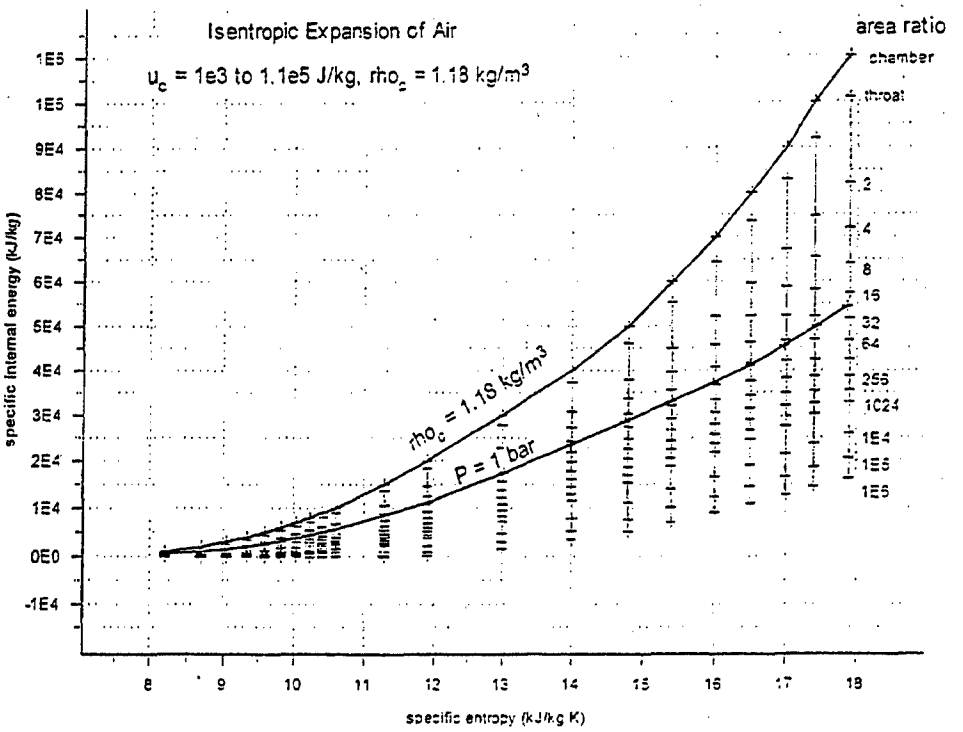

Figure 4. Isentropes for equilibrium expansions originating from the constant density line at 1.18 kg/m^3 and terminating on the constant pressure line at 1 bar. Lines of constant area ratio are nearly coincident with lines of constant density.

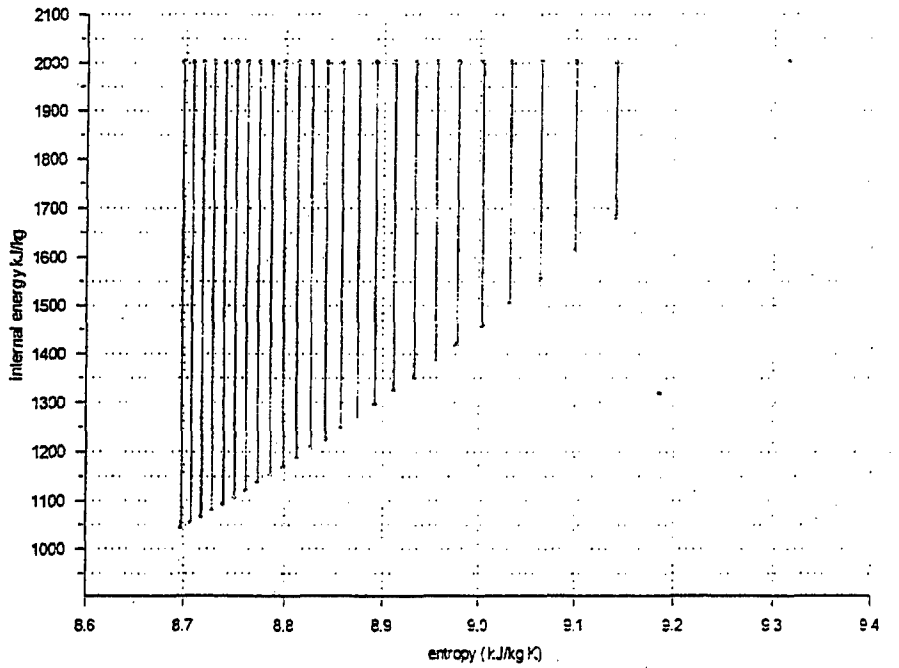

Figure 5. Graphical illustration of computation of blowdown integral from initial state of [u_c-u^o] = 2E3 kJ/kg. The vertical lines are isentropes that are located at equally spaced density increments. The isentropes terminate along the isobar at P = 1 bar.

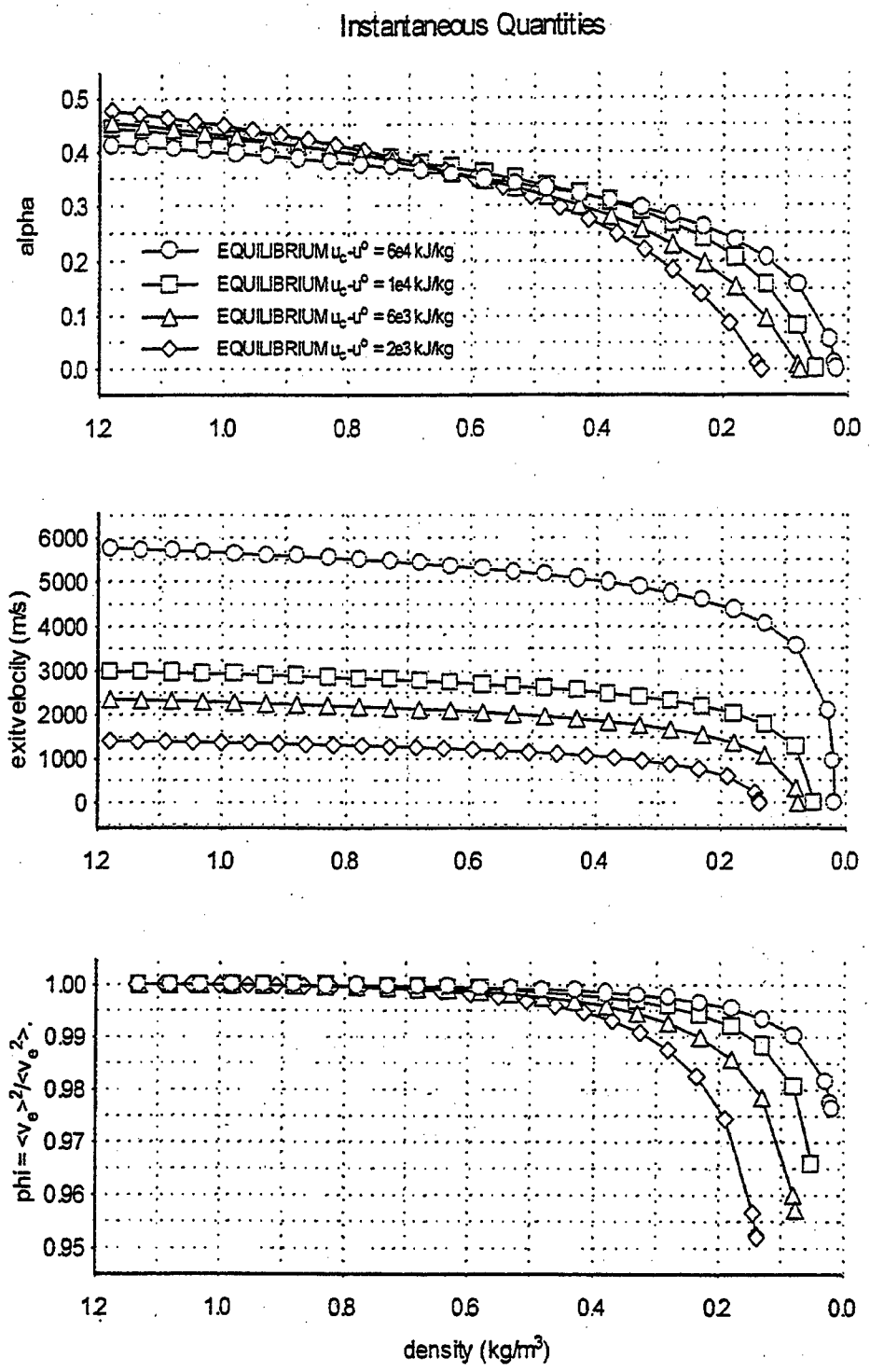

Figure 6. Instantaneous quantities for equilibrium blowdown of heated air from initial density of 1.18 kg/m3 and specific internal energies ranging from 2 to 60 MJ/kg to a final pressure of 1 bar.

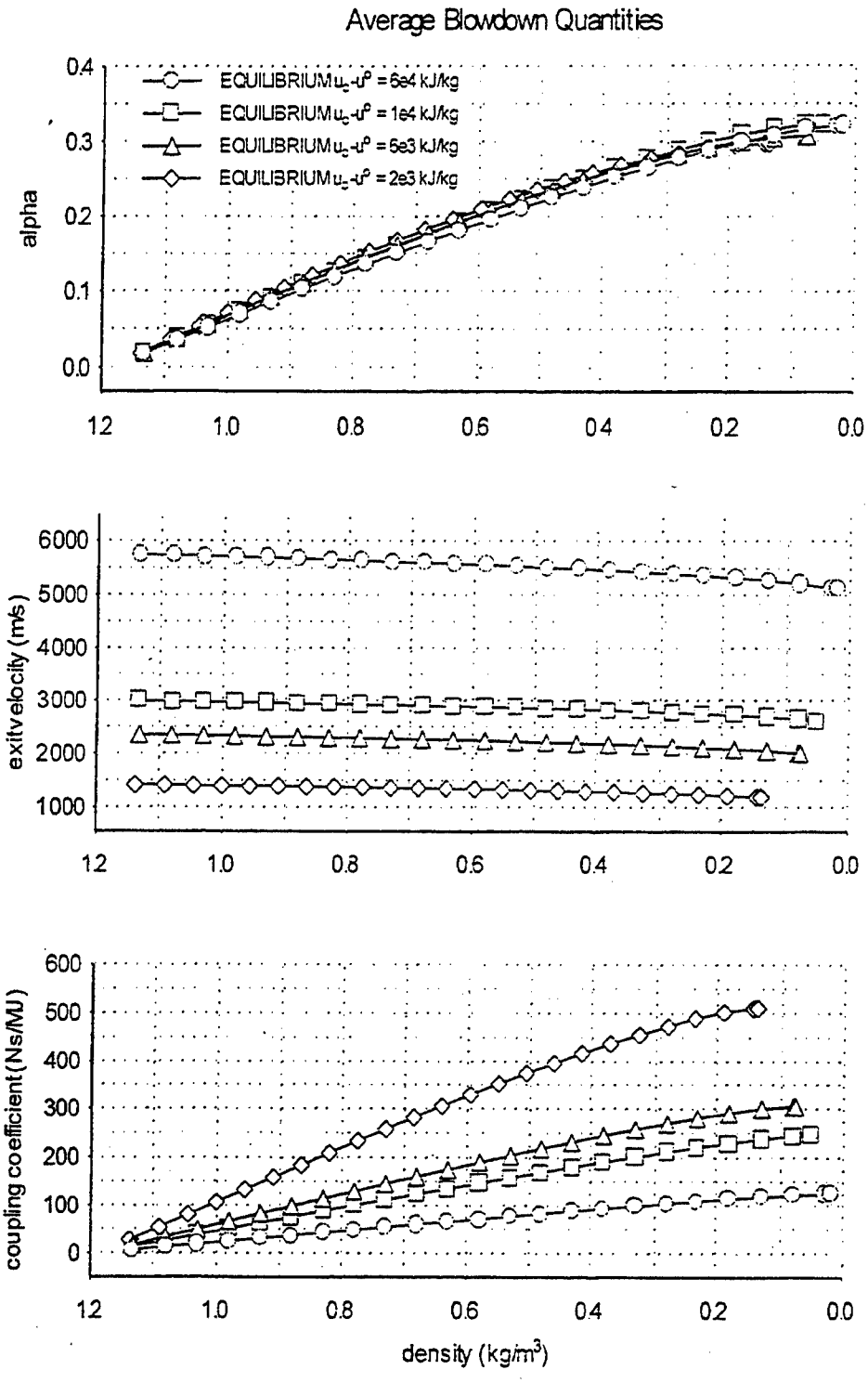

Figure 7. Mass weighted average quantities for equilibrium blowdown of heated air from initial density of 1.18 kg/m3 and specific internal energies ranging from 2 to 60 MJ/kg to a final pressure of 1 bar.

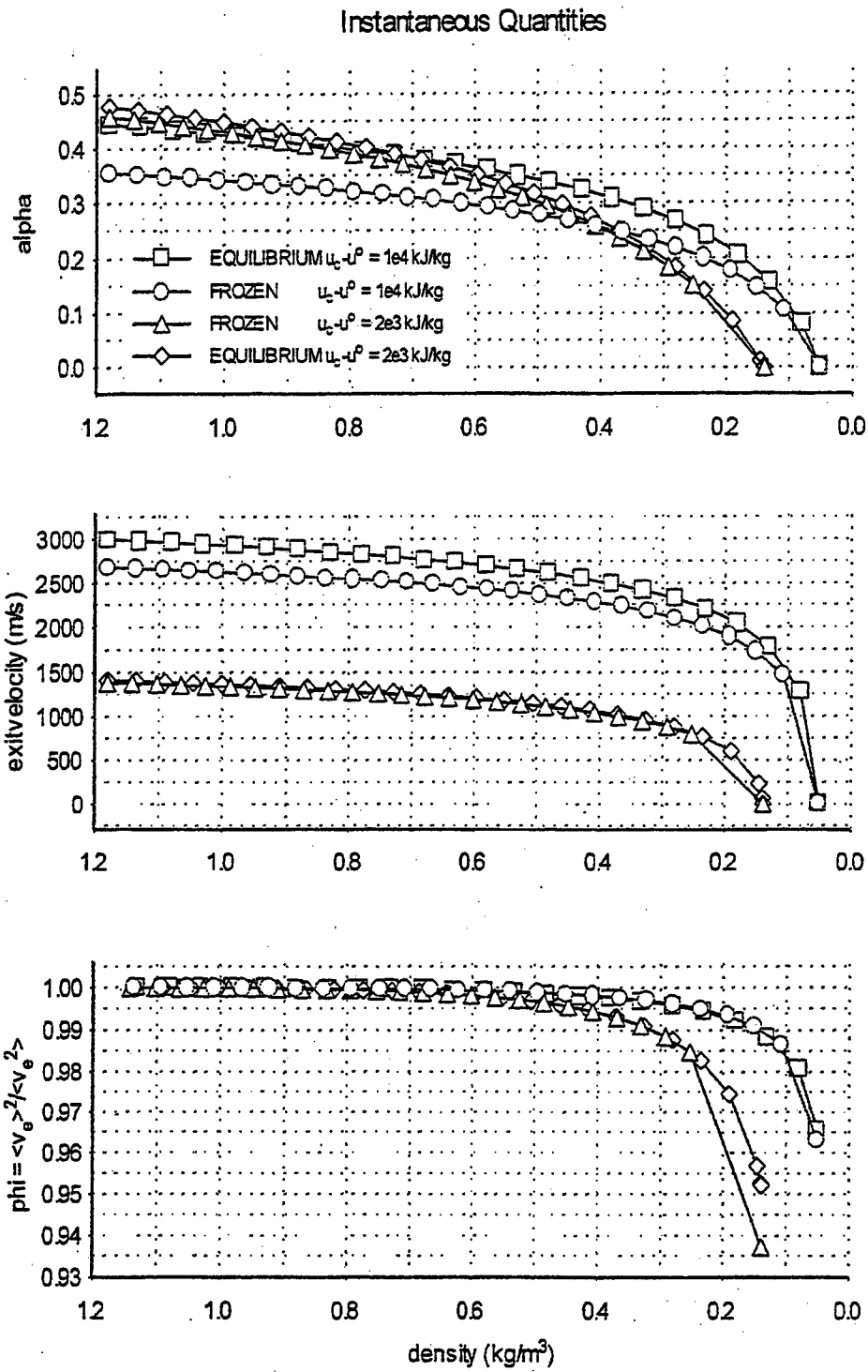

Figure 8. Comparison of instantaneous FROZEN and EQUILIBRIUM blowdown quantities from 2 and 10 MJ/kg initial internal energy. Initial density 1.18 kg/m^3 with blowdown to 1 bar external pressure.

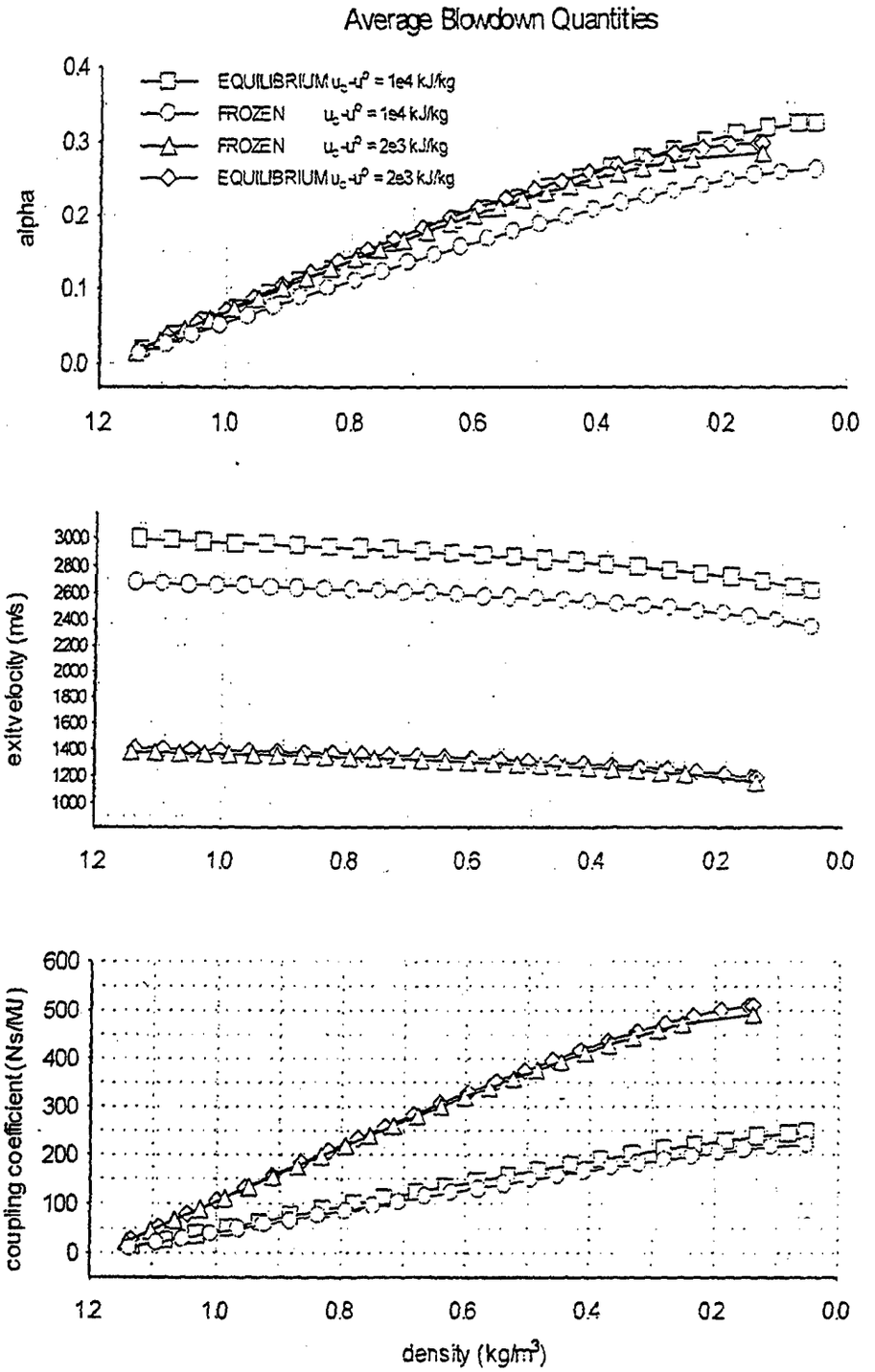

Figure 9. Comparison of mass weighted average FROZEN and EQUILIBRIUM blowdown quantities from 2 and 10 MJ/kg initial internal energy. Initial density 1.18 kg/m^3 with blowdown to 1 bar external pressure.

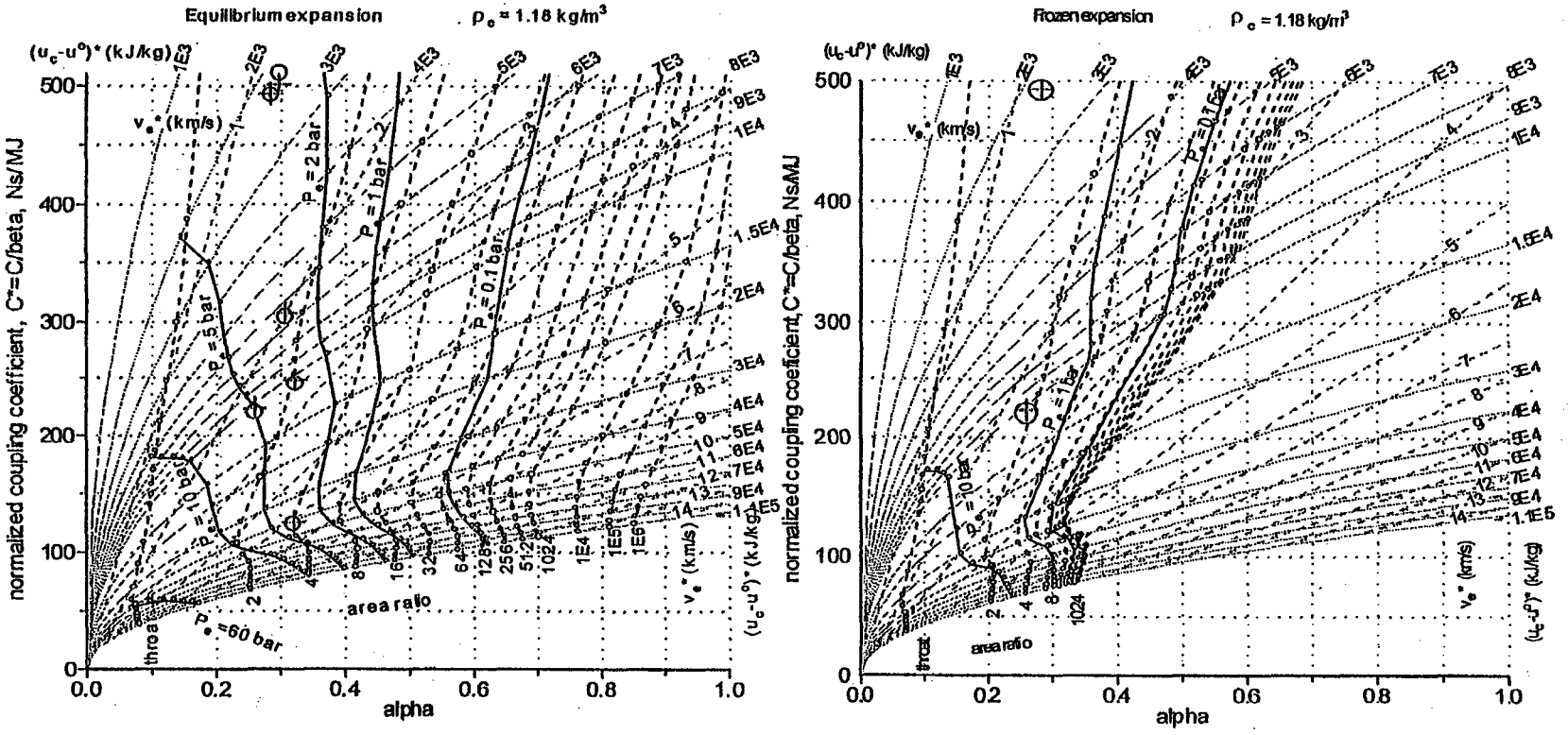

Figure 10. Comparison of Equilibrium expansion and frozen expansion of air. The circles and nearby crosses represent the blowdown quantities obtained from initial $[u_c-u^o]^*$ states of 2E3, and 1E4 J/kg for the frozen expansion and 2E3, 6E3, 1E4, and 4E4 kJ/kg for the equilibrium expansion. The results of the two frozen blowdown integrations to P_{exit} = 1 bar are plotted with those of the equilibrium blowdown to show that the differences in alpha are small, i.e., at low energy (2E3) 0.30 and 0.29 and at high energy (1E4) 0.32 and 0.27 for equilibrium and frozen blowdown, respectively.

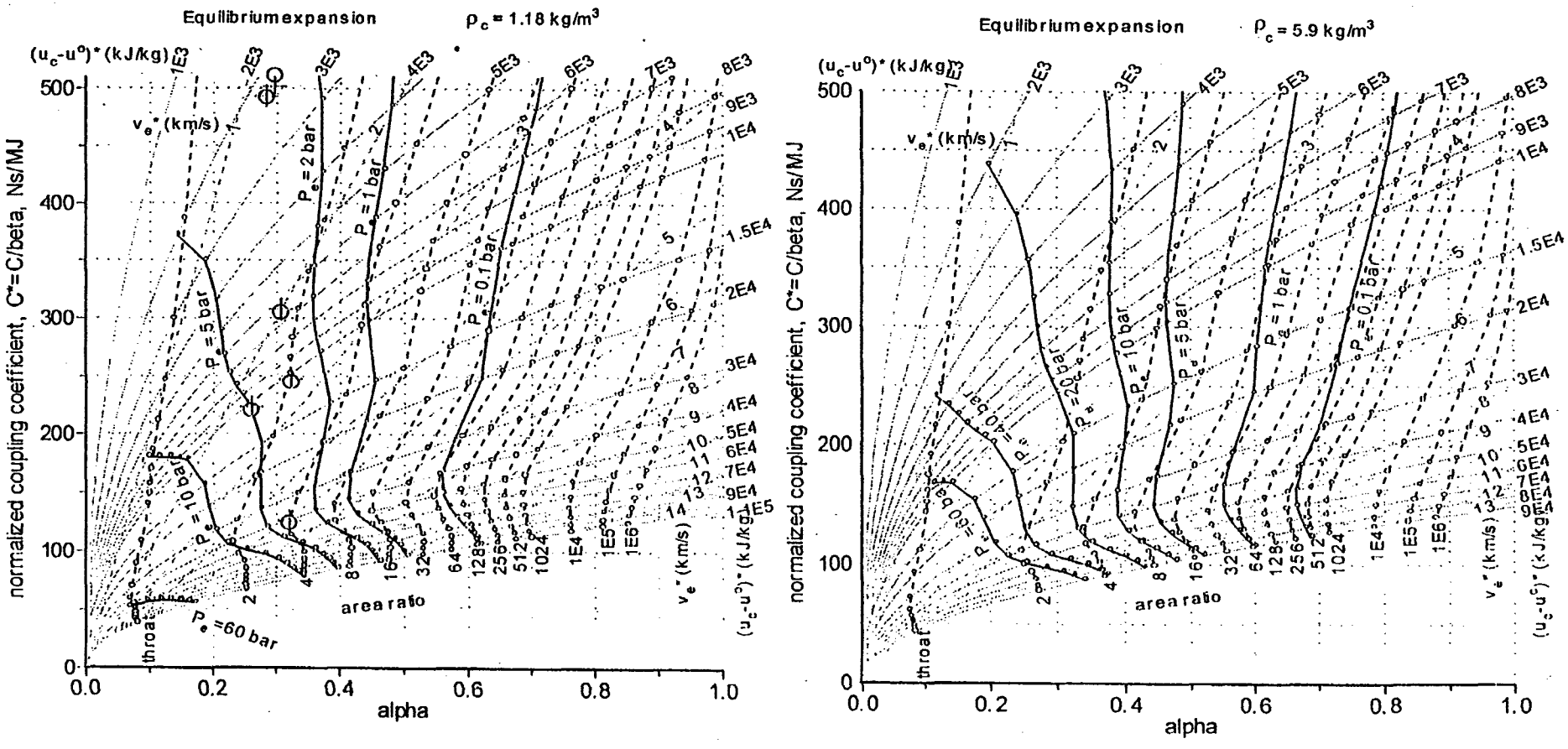

Figure 11. Comparison of Equilibrium expansion from laser heated STP air (1.18 kg/m³) and Mach 5 air at stagnation density (5.9 kg/m³). In the STP air diagram (on left), the circles and nearby crosses represent the blowdown quantities obtained from initial $[u_e-u^o]^*$ states of 2E3, and 1E4 J/kg for the frozen expansion and 2E3, 6E3, 1E4, and 4E4 kJ/kg for the equilibrium expansion.